ISSN 0006-3509, Biophysics, 2017, Vol. 62, No. 6, pp. 950–960. © Pleiades Publishing, Inc., 2017.
Original Russian Text © N.G. Bibikov, S.V. Nizamov, 2017, published in Biofizika, 2017, Vol. 62, No. 6, pp. 1153–1166.

CELL BIOPHYSICS

Evaluation of Postspike Changes in Neuronal Excitability by Comparing Ordinary and Shuffled Autocorrelation Functions

N. G. Bibikov* and S. V. Nizamov

Andreyev Acoustics Institute, Moscow, 117036 Russia

**e-mail: nbibikov1@yandex.ru*

Received April 3, 2017; in final form, June 21, 2017

Abstract—Responses of single neurons to tonal signals amplitude-modulated by repeating segments of low-frequency noise were studied in the dorsal (cochlear) medullary nucleus and midbrain auditory center (torus semicircularis) of the grass frog *Rana temporaria*. An autocorrelation function of the response to a total presentation and a shuffled autocorrelation function were derived. The latter was obtained by correlating the impulse response to each segment of the modulated signal with responses to all other segments with the exception of the initial one. After the necessary normalization, the function differed from the initial autocorrelation only in lacking postspike changes in excitability. A delay dependence of the ratio of the two functions directly demonstrated the time course of the postspike change in excitability of the studied cell. The majority of second-order neurons, which are in the dorsal nucleus of the medulla oblongata, were characterized only by brief intervals of absolute and relative refractoriness. However, cells with excitability that was markedly facilitated immediately after the refractory period were observed even in this nucleus. Neurons with a complex pattern of postspike changes in excitability were detected in the torus semicircularis. In these cells, a comparatively long postspike decrease in excitability was usually interrupted by intervals in which the neuron sensitivity was significantly higher than normal. The results demonstrate that spike generation has a marked effect on subsequent activity in brainstem auditory units. The effects may play an important role in the formation of the temporal pattern of neuronal responses to auditory signals.

Keywords: auditory pathway, refractoriness, shuffled autocorrelation, temporal coding, tailless amphibians

DOI: 10.1134/S0006350917060021

INTRODUCTION

It is only natural to assume that the main function of neurons located in brainstem regions of the direct auditory pathway is to isolate and emphasize the temporal specifics of the auditory signal in certain frequency regions. The mechanisms that allow neurons of the brainstem regions of the auditory pathway to isolate relatively simple primary characteristics of sounds have still not been studied in sufficient detail. To better understand these mechanisms, it is essential to construct an adequate model of the output discharge generation of the neuron. Note that two factors determine the probability of a spike response of a neuron at every fixed point of time; the parameters of the synaptic input that affects the neuron and the internal state of the neuron element itself are the factors. We have long intended to separate these factors, aiming primarily at constructing an adequate model of a neuron [1, 2]. Our previous studies have shown that the internal properties of a nerve cell and, first of all, changes that the mere generation of a spike causes in excitability may substantially affect the response. As an example, a postspike decrease in excitability leads to an effect of short-term adaptation in many cells of the frog auditory system [1, 3, 4]. Model experiments have shown that, when it is actually taking place, an accumulation of postspike decreases in excitability over consecutive spikes may provide a mechanism that sustains short-term adaptation of auditory nerve fibers in mammals [3].

However, it is rather difficult to evaluate the dynamics of postspike changes in a single neuron. Even intracellular recording usually fails to solve the problem because the method does not reflect the character of potentials that occur immediately at the site of spike generation and does not always detect dynamic changes in the spike generation threshold. This may explain why postspike effects receive minor, if any, attention in the majority of auditory preprocessing models. Such models are usually limited to reproducing rather short-term refractoriness without its accumulation or a simple integration–discharge model is utilized, wherein processes associated with memory of preceding discharges are disregarded and a simple monotonic function is used to describe the res-

Abbreviations: ACF, autocorrelation function; SACF, shuffled autocorrelation function.

toration of excitability. This simplified approach is probably partly responsible for the fact that the models that are based on a linear or quasilinear approximation and use data obtained by inverse trigger correlation [5] only poorly reproduce the response of a neuron to new signals [6].

Ample data indicate that postspike changes in excitability play an important role in the neuronal response to sound signals, facilitating a selective response to particular temporal characteristics. A special role is played in adaptation effects, which greatly contribute to the efficient function of the auditory analyzer in a huge dynamic range [3, 4, 7, 8].

We have tried for a long time to quantitatively evaluate the dynamics of postspike changes in excitability of auditory neurons by analyzing their firing activity in the absence of external effects. A hazard function or an autocorrelation function of the process recorded can provide valuable information, given that firing activity is spontaneous and that the neuron under study is assumed to receive no synaptic input [9, 10]. However, the problem of evaluating the dynamics of postspike changes is more difficult in the case of a neuron that lacks background activity and responds only to structured external stimuli.

In this work, we attempted to solve the problem by comparing two correlation functions that characterize the activity of a single auditory neuron exposed to long tonal signals that are amplitude-modulated by repeating segments of low-frequency noise. One function was the autocorrelation function (ACF) of the total sequence of spikes evoked by a long signal. The other function was obtained using a method that was initially designed to analyze the responses to broad-band noise signals consisting of a sequence of fully identical segments [11]. The function is calculated as follows. Once the total sequence of spikes is recorded, correlation functions are constructed for regions of firing activity that arise in response to all different repetitive segments of the signal. The autocorrelation functions that characterize firing activity evoked by each particular segment and produce the ACF when summed are ignored. The number of functions to be summed up for N segments is $N \times (N - 1)$, rather than N, in this case and the resulting correlation function is consequently far more representative than the initial ACF. Its value in the vicinity of a zero delay corresponds to the number of situations where spikes that arise in response to one of the signal segments coincide with spikes that occur in the same time window, but arise in response to any other segment. Thus, a quantitative criterion is set for the extent of synchrony in neuron responses to identical segments of the signal. It is of special importance to note that the function is thought to be absolutely free of the effect of refractoriness because intervals between responses to different segments exceed several hundreds of milliseconds. Although functions of mutual correlation between different modulation segments are actually recorded in this case, the above function is known as the shuffled autocorrelation function (SACF), while the term is not fully correct. The term SACF is used here for convenience, but should not be confused, for instance, with a summary autocorrelation function, which is also mentioned in the literature.

If the ACF and SACF are brought to the same unit of measure by normalization, the ratio of the two functions at consecutive points of time will show the dynamics of postspike changes in cell excitability. This was the objective of our study. Our primary tasks were to estimate the efficiency of the method and to demonstrate that a vast diversity of postspike changes in excitability is observed in neurons of the auditory pathway. A full classification of the cells by this criterion and a detailed comparison of the postspike changes in excitability for different nuclei of the auditory pathway are the subjects of our further research. Preliminary results were obtained in medulla oblongata neurons and were reported in part previously [12].

METHODS

The experimental procedure is only outlined here; its full description is available from our earlier publications [13–15]. Experiments were performed with grass frog *Rana t. temporaria* males (body weight 25–40 g) in autumn and winter. After cold [16, 17] or mild ether anesthesia, a skin fragment and a bone fragment were removed surgically. Wound margins were treated with the local anesthetic lidocaine. The study was performed in compliance with ethical principles of experimental research in cold-blooded animals [18]. Neuronal activity was recorded in frogs immobilized with Alloferin and placed in a special holder with the dorsal side upward in conditions that allow skin respiration.

The firing activity of single neurons was recorded extracellularly using glass liquid electrodes, which were filled with 2–3 M NaCl with a resistance of 3–15 mOhm. A microelectrode amplifier with a high input impedance had a capacitance compensation circuit and allowed the electrode state to be monitored. The signal was further amplified using standard power amplifiers in the 0.3–10 kHz band. Electrode positioning in an auditory nucleus was usually easy to detect by the occurrence of multiple cell activity in response to an irrelevant signal (segments of broad-band noise). Recordings were obtained from two nuclei of the amphibian direct auditory pathway, the dorsal nucleus of the medulla oblongata and the principal nucleus of the torus semicircularis. Acoustic signals were delivered to the tympanic membrane from a dynamic telephone via a closed acoustic transmission line and were controlled using a calibrated condenser microphone with an adaptor. Stimuli were presented to the ipsilateral tympanic membrane when studying the dorsal nucleus (an analog of the mammalian ventral cochlear nucleus) and to the contralateral mem-

brane when studying the torus semicircularis (a homolog of the mammalian colliculi inferiores).

Once the electrode entered the auditory zone, its vertical displacement was performed distantly with 4-μm increments. Recording started after detecting spikes of a standard shape that were generated by a single neuron and were 5–20 times higher in amplitude than multiple cell noise. After detecting a single neuron, test tonal segments of 100–200 ms in duration were presented to determine the tone frequency that caused a response at the minimal signal level (a characteristic frequency) and the response threshold at the given frequency.

In the main study, frogs were presented with long characteristic-frequency tones that were amplitude-modulated by repeating segments of low-frequency noise. Modulation was performed using a G-110 sinusoidal generator, which had a special input for performing amplitude modulation. A modulating signal was delivered from the output of a G5-57 noise generator, which generated repetitive segments of a constant shape. The signal with constant parameters was usually 100 or 200 s in total duration; the repetitive segments varied in duration from one fourth of a second to more than 2 seconds.

Three different frequencies (15, 50, and 150 Hz) were used as an upper cut-off frequency of modulating noise. Three actuation types were possible for each band, which differ in the shape and duration of the repetitive segment. All actuations of the modulating noise function that were the same in duration and noise band were identical. The extent of modulation was measured as percent mean-square ratio of the modulating noise to mean tonal signal. The ratio was usually 20–30% to avoid overmodulation.

The signal recorded with the amplifier was transmitted to a pulse former, which generated standard pulses corresponding to each spike of the neuron under study; the pulses were stored on a PC. The input from another pulse generator to the PC included synchronization pulses, which marked the starts of identical segments in the modulating signal. The distribution of between-pulse intervals in the response and a time course of the mean neuron firing rate, which was recorded once in every 2 s, were obtained during the experiment. The latter function was used to verify that abrupt uncontrollable changes do not arise in the neuronal response during recording. The cell response was usually recorded starting 10–25 s, rather than immediately, after the start of a stimulus to allow the response to approximate a steady state.

After the experiment the file with a total spike sequence was divided into fragments corresponding to the duration of the fixed noise segment that was employed in modulation. The number of fragments depended on the total duration of a recording and the duration of each segment, varying from 50 to 250. As an example, Fig. 1a shows the shape a 1012-ms envelope fragment with a modulating function range of 0–50 Hz. Unity and –1 correspond, respectively, to the maximum and minimum amplitude observed for the modulation segment. The first step of data processing was the construction of pulse distribution histograms known as cyclic histograms for the modulation noise segment. An example histogram is shown in Fig. 1b.

A nonnormalized ACF was constructed for the total actuation duration according to the following equation:

$$\mathrm{ACF}(T) = \Sigma x(t)x(t + T)dt.$$

An SACF was constructed by dividing the response to the total presentation into fragments that correspond to one period of the modulating function and counting the cases where the start of firing in response to a particular segment of the modulating function coincided with the start of firing in response to all other segments. As mentioned above, the number of such segments was $N \times (N - 1)$. A histogram of an SACF was obtained by summing all of the resulting functions.

Both the SACF and ACF were normalized so that the mean parameters of fully independent firing segments that were to be compared corresponded to the mean firing rate. For this purpose, the number of coincidences observed at a particular delay was divided by the total segment duration, the width of a single shift, and the mean firing rate when constructing the ACF and, additionally, by the number of segments minus unity when constructing a time-shuffled autocorrelation function. Normalization yielded the two functions expressed in the same units of measure, that is, current firing density and could be compared directly.

A histogram of the ACF is shown in Fig. 1c. Its value in the zero channel, which corresponded to a unity probability and was 2000 at the single sampling duration 0.5 ms used in the experiment, is omitted. The function is zero at small delays because a neuron that has generated a spike is unable to immediately generate another one as a result of what is known as absolute refractoriness. Starting from a delay of 1.5 ms, the function gradually increases as refractoriness is eliminated and then decreases to a level corresponding to the mean firing rate.

A histogram of the SACF (Fig. 1d) has a maximum at a zero delay, which corresponds to the probability of a spike to arise in the same position in various segments of the modulating signal. Note that the ratio of the maximum to the mean firing rate directly demonstrates the extent of synchrony for responses obtained to consecutive presentations of the same signal segment. The ratio has been proposed for use as a synchrony index or coefficient [15, 19]. Note additionally that the SACF appears to be far smoother than the ACF, with the difference being due to the large size of the dataset used in comparisons.

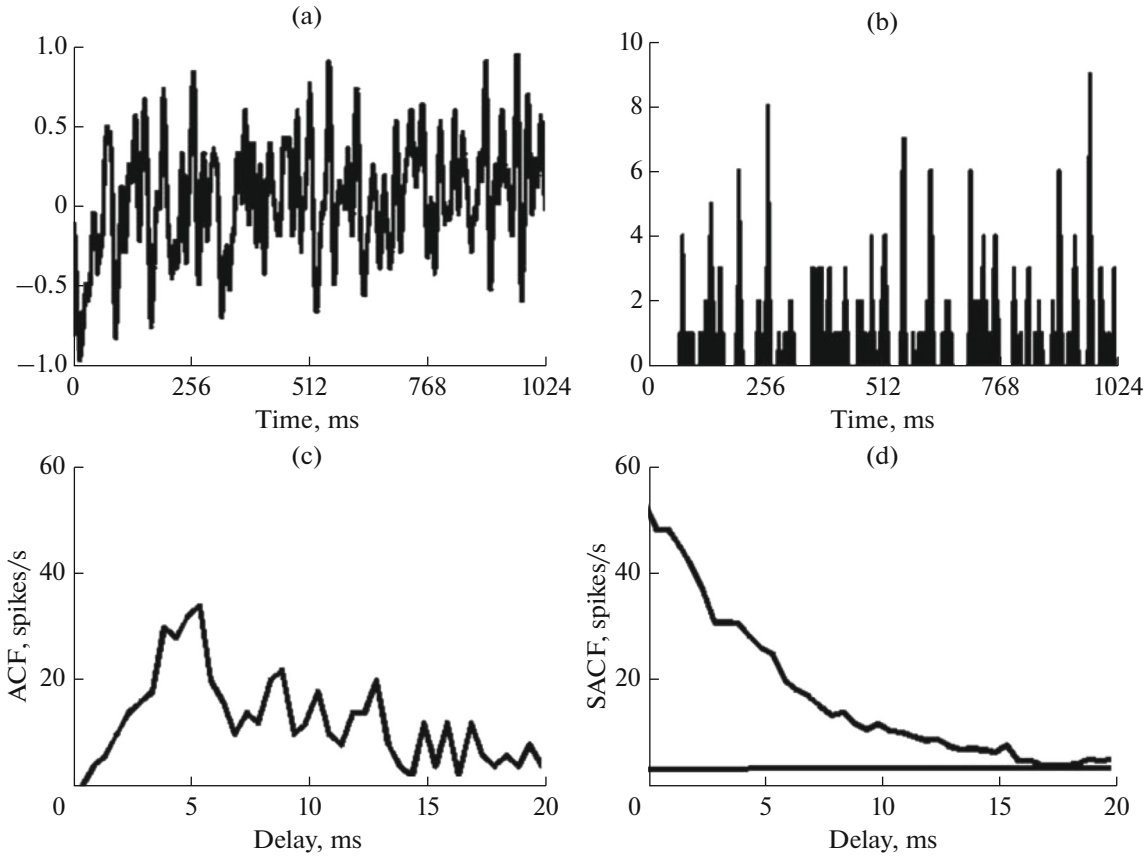

Fig. 1. The response of a typical neuron of the torus semicircularis to a characteristic-frequency signal modulated with repetitive 1024-ms noise segments in the band 0–50 Hz. (a) The normalized shape of an envelope fragment. (b) Cyclic histogram of the response to the fragment. (c) Histogram of the autocorrelation function constructed for the total actuation duration. (d) Histogram of the shuffled autocorrelation function obtained by comparing the responses to different segments of the modulating signal. The mean firing rate is shown with a horizontal line.

We analyzed the ACF-to-SACF ratio for each consecutive delay of correlation functions. The ratio characterizes the process whereby excitability of a neuron changes because the neuron has generated an action potential (a spike). When experiments with one neuron are performed using different signal parameters the dependence of the ratio on the time after spike generation must be nearly constant, being determined by internal properties of the neuron. This feature makes it possible to sum up such dependences and to obtain their mean and standard deviation. These procedures were performed using the standard Excel and Origin programs.

RESULTS

In total, we examined more than 40 neurons of the dorsal nucleus and more than 100 cells of the torus semicircularis. The study included only the neurons that showed a stable response to optimal-frequency tonal signals amplitude-modulated with low-frequency noise by 20–30%. A detailed quantitative analysis of the total dataset is beyond the scope of this work. Our primary objective was to demonstrate that the method is efficient and that substantial diversity of postspike changes in excitability is characteristic of neurons of the auditory pathway.

Cells with weak postspike effects were observed in both the dorsal nucleus of the medulla oblongata and the torus semicircularis. Figure 2 shows the main characteristics of two torus semicircularis neurons of the group. Three SACFs obtained at different ranges of the modulating signal are shown at the top and ACFs normalized similarly are shown in the central row. The ratio of the two functions is shown at the bottom (the solid line shows the average ratio). The neurons differed in characteristic frequency (0.50 and 0.83 kHz, respectively) and especially in the average firing rate (0.50 and 28.3 spikes/s, respectively, in response to a signal modulated in a band of 0–15 Hz). Both of the neurons displayed a short (approximately 1 ms) absolute refractoriness, a similarly short relative refractoriness, and an ACF-to-SACF ratio that was maintained close to unity afterwards. Note additionally that the periodicity of the ACF can be seen in the responses to low-frequency modulation for the neuron

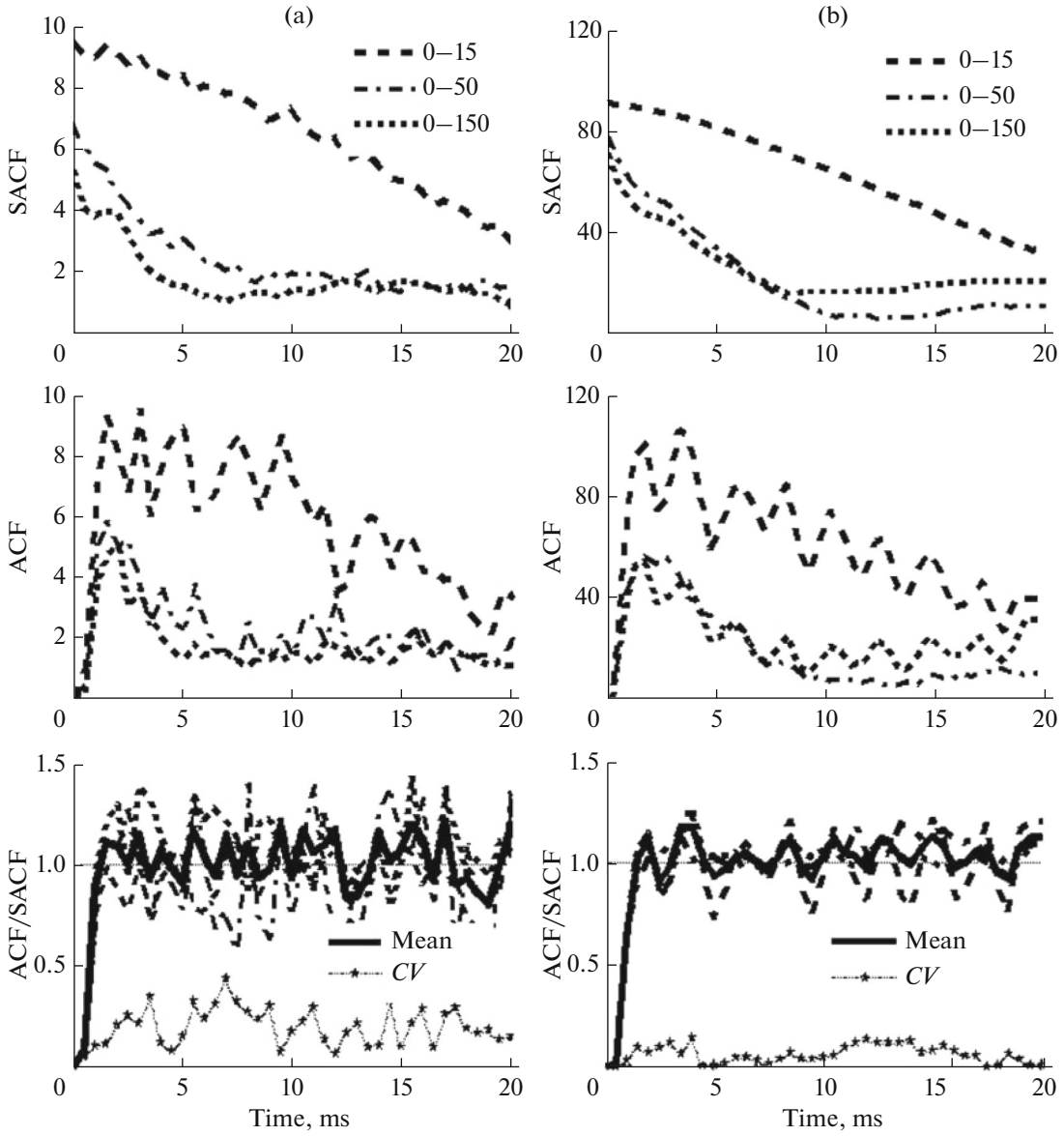

Fig. 2. The characteristics of the firing activity in two neurons of the torus semicircularis in response to characteristic-frequency signals modulated by repeating noise segments. The shuffled autocorrelation functions are shown in the upper row; the autocorrelation functions are in the central row. The lower row shows the ACF-to-SACF ratios for three signals with different ranges of the modulating signal, as well as their mean values and standard deviations (CV). (a) Neuron 91102: carrier frequency, 0.5 kHz; mean signal intensity, 30 dB over the threshold; mean-square modulation depth, 20%. (b) Neuron 62001: carrier frequency, 0.83 kHz; mean signal intensity, 30 dB over the threshold; mean-square modulation depth, 20%. The modulation parameters shown at the top right corner pertain to all plots for the respective neuron.

with a higher firing rate (Fig. 2b). This feature is probably related to the fact that the neuron had a high, although short, refractoriness and consequently produced pairs of spikes with a strictly defined between-spike interval. The time points at which such pairs started slightly varied among responses to consecutive segments of the signal; as a result, the effect was seen in the ACF and was virtually undetectable in the SACF.

A reasonable question that occurs during the analysis of our data is whether the postspike effects remain constant when parameters of the signal change. If our method is adequate for evaluating the dynamics of postspike changes in excitability then the shape of the ACF-to-SACF function will not strongly depend on the signal type. The results showed, in fact, that the function did not change qualitatively with changes in modulation range (Fig. 2).

The results for neurons of the dorsal nucleus support the conclusion that the ACF-to-SACF ratio remains qualitatively stabile upon changes in signal parameters. Figures 3a and 3b show the average results

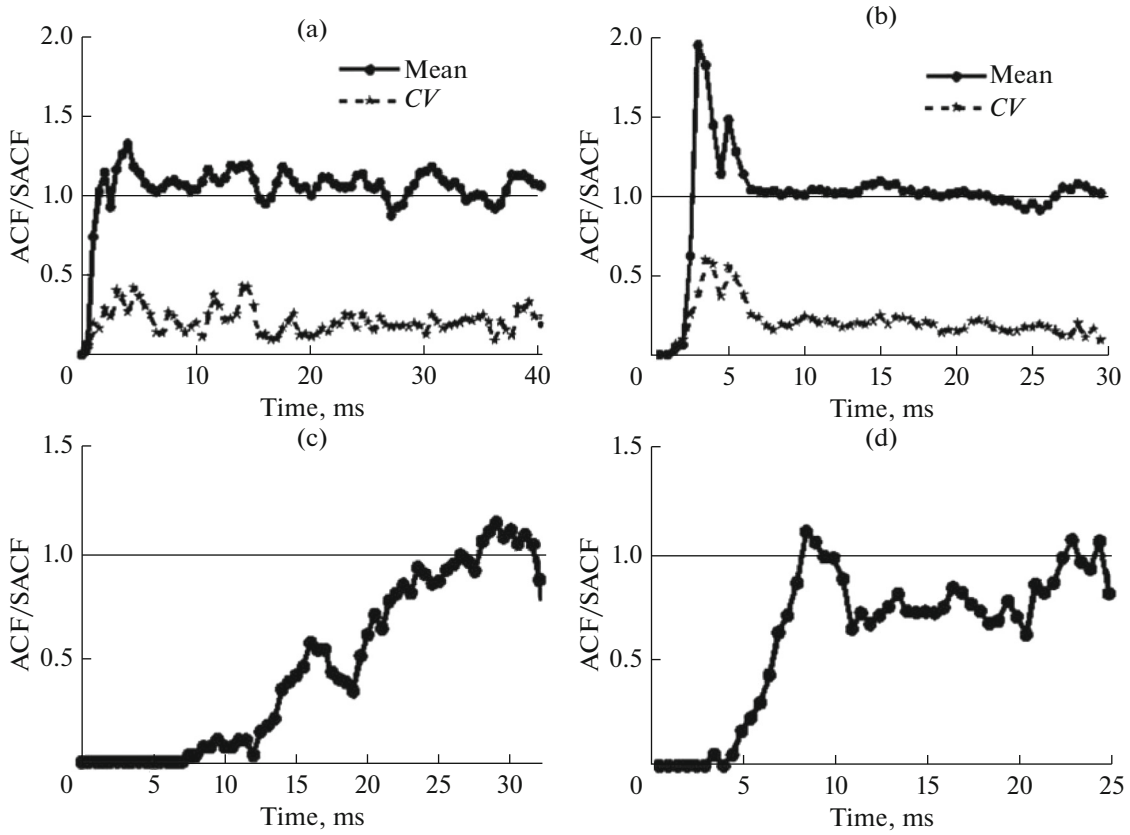

Fig. 3. Functions that characterize the ratio of the common autocorrelation function to the shuffled autocorrelation function as averaged over different signals. The functions were obtained for (a), (b) two neurons of the dorsal nucleus of the medulla oblongata and (c), (d) two neurons of the torus semicircularis with characteristic-frequency signals modulated by repeating noise segments. (a) Neuron 91303: carrier frequency, 0.53 kHz; averaging over the reactions to nine different signals. (b) Neuron 62105: carrier frequency, 1.2 kHz; averaging over the responses to 12 different signals. (c) Neuron 90401: carrier frequency, 0.64 kHz; mean signal intensity, 20 dB over the threshold; mean-square modulation depth, 30%. (d) Neuron 60910: carrier frequency, 1.28 kHz; mean signal intensity, 30 dB over the threshold; mean-square modulation depth, 20%.

that were obtained for two dorsal nucleus neurons with relatively short postspike effects. The data that were averaged to obtain the functions were collected with signals that differed not only in modulating frequency band, but also in carrier frequency and segment length. Although substantial differences were observed in firing rate and the shape of cyclic histograms of the responses to signals presented (data not shown), the time course of the ACF-to-SACF ratio remained qualitatively the same. One of the neurons (Fig. 3a) quickly restored its excitability after generating a spike and its function was otherwise unremarkable. In the case of another neuron (Fig. 3b), the function showed two local maxima immediately after the refractory period of approximately 2 ms; the excitability gradually decreased to unity. Note that a qualitatively similar, although not as distinct, effect can be observed in Fig. 3a. The mean-square deviation was additionally calculated for the two neurons based on their responses to 9 (Fig. 3a) or 12 (Fig. 3b) different signals. The variation approximately corresponds to a common binomial distribution and follows changes in the mean value.

The above neurons relatively quickly restored their excitability after a short refractory period or a relatively short period of a higher excitability. However, such cells were not in a considerable majority, even in the dorsal nucleus of the medulla oblongata and constituted only a minor portion of neurons in the torus semicircularis. Other torus semicircularis cells displayed not only the above postspike effects, which lasted only a few milliseconds, but also other, longer changes in excitability after generating their own spikes.

Some torus semicircularis cells showed an extremely long period of a lower excitability after generating a spike. An example curve of excitability restoration in such a neuron is shown in Fig. 3c. The ACF of the neuron totally lacked intervals of less than 7 ms. The further restoration of excitability was rather slow; it took at least 30 ms for the neuron to fully restore its excitability after generating a spike. In the case of another neuron (Fig. 3d), excitability restored rather

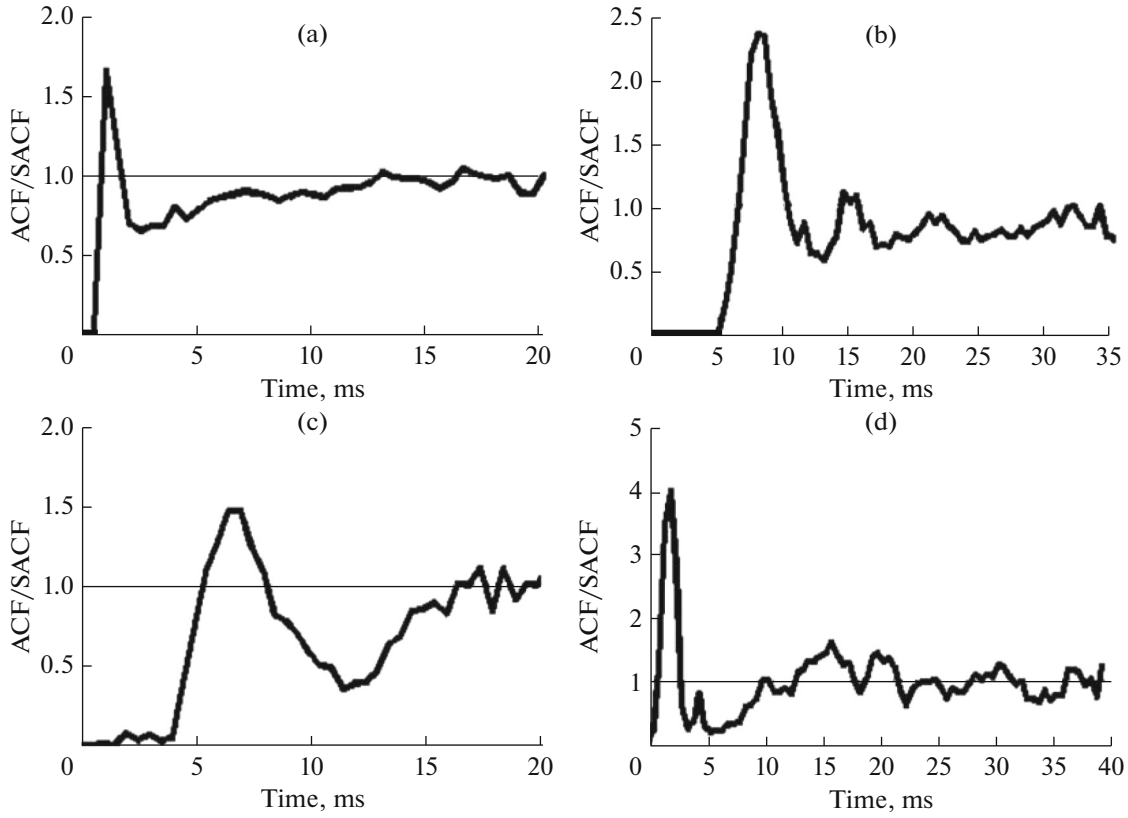

Fig. 4. Functions that characterize the ratio of the common autocorrelation function to the shuffled autocorrelation function in the responses of four torus semicircularis neurons with a nonmonotonic time dependence of excitability after spike generation. (a) Neuron 50406: carrier frequency, 0.6 kHz; mean signal intensity, 30 dB over the threshold; mean-square modulation depth, 20%. (b) Neuron 60607: envelope band, 0–50 Hz; carrier frequency, 1.14 kHz; mean signal intensity, 20 dB over the threshold; mean-square modulation depth, 20%. (c) Neuron 61813: envelope band, 0–150 Hz; carrier frequency, 0.64 kHz; mean signal intensity, 30 dB over the threshold; mean-square modulation depth, 20%. (d) Neuron 62109: carrier frequency, 0.8 kHz; mean signal intensity, 30 dB over the threshold; mean-square modulation depth, 30%.

slowly again, but the nonmonotonic character of the process was even more distinct than in the case of the previous neuron (Fig. 3c). Neuron excitability was restored within 8–10 ms postspike and decreased again at higher delay values.

This complex pattern of postspike restoration of excitability was observed for many neurons of the torus semicircularis. A period corresponding to a facilitation of the response immediately after the end of the refractory period (as shown for a medulla oblongata neuron, Fig. 3b) was observed for many auditory neurons of the midbrain. A primary maximum was often followed by a secondary minimum with subsequent slow restoration, as is seen in Figs. 3c and 3d. The exact time points and the extent of particular components corresponding to various regions of the nonmonotonic function greatly varied.

Figure 4 shows the behaviors of four torus semicircularis neurons with dramatic postspike changes in excitability. In the case of one neuron (Fig. 4a), a region corresponding to a facilitation of the response followed a period of absolute refractoriness and was extremely short; the subsequent decrease in excitability was not very high, but was long, lasting more than 10 ms. All of these phases of postspike changes in excitability were far more distinct in the other three neurons; region of a higher excitability could be as long as several milliseconds (Fig. 4b). Two neurons (Figs. 4c, 4d) demonstrated again that the epoch of a secondary postspike decrease in excitability can be rather long and that the restoration of excitability can be nonmonotonic. Secondary maxima seen in Figs. 4c and 4d were observed in other cases as well.

In some cases, the time course of excitability restoration could not be characterized in full because SACF values rapidly decreased to zero in the initial region, while ACF values were zero at low delays, when SACF was nonzero. This situation was observed for the cells that responded via a single spike only to certain extremely short fragments of the signal. As we have previously shown [15], these elements were characterized by an extremely high synchrony coefficient and a rapid decrease of SACF to zero. Such behavior corresponds to the coding type known as sparse coding,

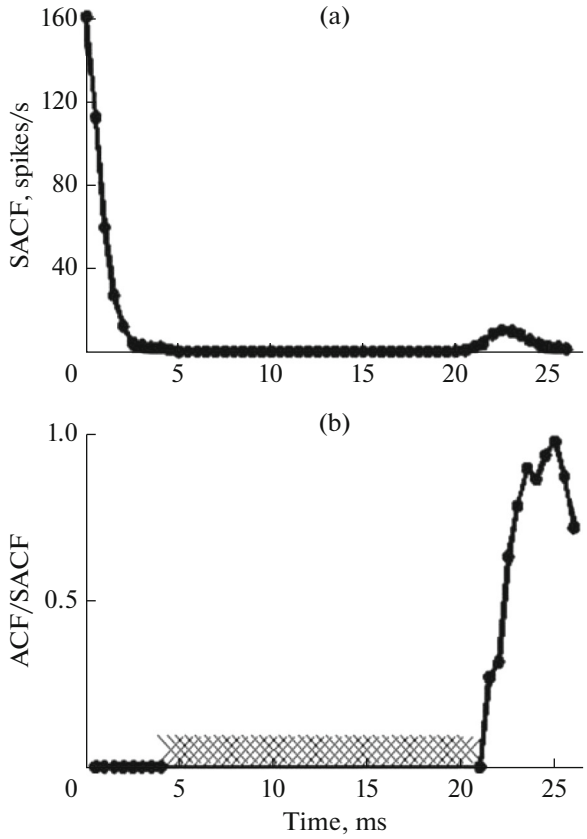

Fig. 5. Functions that characterize the response of a torus semicircularis neuron (neuron 61303), which produced a short-term response only to particular envelope regions. (a) A shuffled autocorrelation function averaged over three tonal signals modulated with noise of the range of 0–150 Hz. The carrier frequency and the characteristic frequency of the neuron were 0.67 kHz. The parameters of the three signals: the carrier signal intensity of 20 dB over the threshold with an extent of modulation of 20 or 30% and the carrier signal intensity of 30 dB over the threshold with the extent of modulation of 20%. (b) The ratio of the common autocorrelation function to the shuffled autocorrelation function for the same cell. The ratio is undefined within the 5–25 ms interval because both of the functions are zero.

wherein only a minor number of neurons are involved in the response to a particular signal in a neuronal population, with each isolating its own characteristic feature of the signal.

The results for one such neuron are shown in Fig. 5. The SACF (Fig. 5a) was obtained for the response to a signal modulated with an envelope band of 0–150 Hz. The function had an extremely high maximum at minimal delays and then rapidly decreased to zero. A small secondary maximum in the region of 22- to 24-ms delays corresponded to the interval between two envelope features that led to a spike. The ACF-to-SACF ratio averaged over the three signals in question is shown in Fig. 5b. The ratio is zero over the first 4.5 ms and is undefined in the 4.5–21 ms interval because the two functions are equal (or extremely close) to zero. However, the ratio approximates unity at delays of 22–25 ms, which correspond to the interval between two signal features that evoke firing activity (Fig. 5b). When lower envelope frequency bands were used, zero ACF values corresponded again to a primary SACF maximum and the delays of the secondary maxima were even greater.

DISCUSSION

Naturally, the results of this work were compared with our previous attempts to characterize the dynamics of postspike changes in excitability in the same elements of the amphibian auditory pathway. The extent of excitability restoration has been evaluated by studying the probability for a neuron to respond to the second click in a pair as dependent on whether a spike was generated in response to the first click [20]. The intervals between the first and second clicks were 20, 40, 60, or 100 ms. When the interval was the shortest, the response to the second click was suppressed in the majority of cells given that a spike was generated in response to the first one. With 40- and 60-ms intervals, we observed not only this interaction type, but, sometimes, also an effect where the probability of responding to the second click increased in the presence of a response to the first one. As was mentioned in that work, the portion of cells with a distinct effect of a previous spike on the probability of a second response could be underestimated because of the limitations imposed by the method. The limitations arose because it was essential to clearly distinguish firing activity evoked by the first click from that to the second one and to obtain a sufficiently representative set of reactions where a response to the first click was absent. Moreover, cells that generated more than one spike in response to a click were excluded from the analysis. It is possible to assume that cells with distinct poststimulus or postspike inhibition were thus selected, while postspike facilitation, which usually develops at short delays, was far more difficult to detect.

A study that was similar in approach was carried out in neurons of the midbrain auditory center in mice [21]. The signal consisted of a pair of short tonal segments and results were collected at constant between-stimulus intervals of 50 ms or a longer duration. Even with these long between-stimulus intervals there were cases where the probability of responding to the second signal was substantial in the absence of a spike to the first one and zero in its presence. However, neurons that increased in excitability after generating a spike in response to the first signal were also observed. One of these neurons displayed the property even when the between-stimulus interval was as long as 200 ms.

In another work, we attempted to infer the time course of postspike restoration of excitability directly

from the responses of neurons to tonal segments [22]. The distribution of the starting points of all spikes relative to the start of the signal (a poststimulus histogram) was compared with an expected firing density histogram [23], which shows a hypothetical temporal distribution of spikes generated in response to a signal in the absence of refractoriness. The latter histogram was calculated from a sufficiently representative distribution of response latencies observed in the absence of spontaneous activity. The data used with the analytic model made it possible to evaluate the dynamics of excitability restoration, but only with highly simplified assumptions made in the model for the temporal parameters of the process. It was assumed that one absolute refractoriness period exists; its duration was the only variable parameter. The analysis under these assumptions demonstrated again that neurons of the grass frog midbrain auditory center greatly vary in the duration of total postspike inhibition. The parameter had almost no effect on the course of a response in some cells, while its duration estimated with the above simplified model reached 20 ms in some other neurons. The results of our current work also demonstrate that a long postspike inhibition period is characteristic of a limited and probably specialized group of midbrain neurons.

To summarize the comparison of our results with data from other studies performed with the same models and the same purpose, a long aftereffect of spike generation was observed for some neurons in previous studies and confirmed in this work. The method proposed in this work made it possible not only to demonstrate the effect, but also to characterize its temporal dynamics.

In the case of neurons with distinct spontaneous firing activity, its autocorrelation function or hazard function are certainly suitable for studying these processes [9, 24]. However, the majority of neurons of the midbrain auditory center do not generate spikes in the absence of an external signal in both amphibians and mammals. Moreover, the mere generation of spike activity does not mean that the cell receives no input, which can originate from other sources and can be arbitrarily complex in organization. Although input unrelated to external signals cannot be fully excluded, the method used in this work must be less sensitive to such influences because the firing activity to be recorded is determined mostly by the external signal, which is identical for both SACF and ACF.

The dynamics of postspike changes in excitability and restoration of auditory neurons after exposure to sound stimuli have not been characterized in detail in the available literature. However, our results are not in conflict with data reported in other studies. A direct comparison of the SACF and ACF obtained for the total actuation has been performed in a study of the cat auditory nerve (see Fig. 3 in [11]). The comparison was poorly qualitative and was not aimed at evaluating the total time course of postspike changes in excitability of a neuron. The maximum seen in the common ACF immediately after the refractory period (at a delay of 2 ms) was approximately the same as the SACF value at the same point, i.e., refractoriness was extremely short in duration, and only a weak, if any, facilitation of the cell response occurred after the end of the refractory period. This pattern is similar to the patterns of the neurons characterized in Figs. 2 and 3a. However, far longer and more complex changes in excitability can be induced in auditory neurons by spike generation, as is evident from our results and especially those obtained for midbrain neurons.

A postspike decrease in excitability that differs from the classical pattern described by the Hodgkin–Huxley model is widespread in brain neurons and, in particular, neurons of the brainstem regions of the auditory system. The mechanisms of the effect have been studied in both neurons of the auditory system and other brain structures. The effect is usually explained by the function of calcium-activated potassium channels, which are classified into two subgroups. Large-conductance channels, which may be found in the initial segment of the axon [25], act within several milliseconds after spike generation, while small-conductance channels may have far greater time constants [26]. In our case, a decrease in excitability, which is seen, for example, in Figs. 2 and 3a, can presumably be attributed to the function of large-conductance channels. The function of small-conductance calcium-activated channels may be responsible for slower changes in excitability, such as those shown in Figs. 3c, 3d, and 4.

We note that the two currents that hyperpolarize the cell are additive in nature; i.e., they are capable of accumulating over consecutive action potentials. It has long been noted that these accumulating currents can explain the important phenomenon of short-term adaptation in auditory nerve fibers [3]. However, an integrate-and-fire approach is used to reproduce the postspike changes in excitability in the majority of models, i.e., the spike effects on the neuron state at a given time point are fully ignored for all but one spike of the neuron, with the spike that immediately precedes the time point being the only exception.

A local maximum of the ACF-to-SACF ratio, which was observed for many cells examined, can be determined by several basically different factors. A true increase in excitability of the neuron is highly likely to occur immediately after spike generation and subsequent fast refractoriness. Many ionic mechanisms can be responsible for the effect. One of the possible mechanisms of postspike depolarization has been considered, particularly for auditory neurons of the mammalian brainstem [27]. Sections of neurons of the medial nucleus of the trapezoid body have demonstrated the existence of the so-called resurgent temporal sodium current (I_{NaR}), which is activated during

membrane repolarization after an action potential. The same currents are possibly responsible for burst activity of the so-called cartwheel cells of the dorsal cochlear nucleus in mammals [28].

Other mechanisms of postspike depolarization are possibly related to rebound depolarization following postspike hyperpolarization [29] or a temporal suppression of outward potassium currents [30]. These processes are similarly triggered by inward calcium flux.

Mechanisms other than actual facilitation may also contribute to the maxima of the function, which was used to characterize a postspike restoration of excitation in this work. The maxima may seem to arise because the input frequency is low and, on average, the signal amplitude consequently remains higher than average after the generation of the first spike. However, this effect must be reflected in the SACF as well, widening the initial peak. Such a widening actually takes place, and the duration of the initial SACF peak increases with the decreasing upper frequency limit of the modulating function [15]. Therefore, this factor cannot explain a substantial increase in ACF over SACF. In fact, we did not observe the restoration function to considerably depend on the bandwidth of the modulating noise (Figs. 2, 3).

It is possible to assume that the responses to consecutive presentations of the same noise envelope greatly vary, so that enhanced responses with a higher frequency of pairs of closely spaced spikes are evoked by some presentations. The SACF derivation procedure eliminates these features and consequently decreases the number of corresponding intervals. A local increase in ACF values over SACF values may arise as a result. We assume a greatly simplified situation where a pair of spikes with a constant interval is generated in response to half of the presentations, while the other presentations fail to evoke any response. A substantial increase in ACF values over SACF values will be observed in the range corresponding to the between-spike interval of the spike pair in this case.

There are grounds to believe that a chaotic variation of responses to consecutive signal presentations is characteristic in fact of neurons of the auditory system. Studies of the spontaneous activity of neurons of the auditory pathway in amphibians have clearly demonstrated that slow chaotic fluctuations occur in neuronal excitability and are seen, in particular, as a disproportionate dramatic increase in Fano factor (a ratio of the variance to the mean of spike counts) with the increasing length of the epoch under study [31]. The variation of responses to repetitive signal segments is additionally possible to assess using a relatively simple parameter, which corresponds to the Fano factor and is the ratio of the variance of the spike counts in the responses to a signal segment to the mean number of responses to the signal. We have previously shown that the ratio can substantially exceed unity when isolated tonal segments are used; i.e., chaotic changes exist, in fact, in responses to consecutive signal presentations. In the context of the problem addressed in this work, this parameter should be evaluated by treating consecutive modulation segments as individual segments. A comparison of the parameter with the excitation restoration curves may help to better understand one of the possible factors that is responsible for local maxima.

A periodicity that exists in neuron responses and is unrelated to the period of modulating segment presentation is another factor that can explain the ACF increase over the SACF at certain delays. The effect is most clearly seen when the cell reproduces the periodicity of the carrier frequency. Such a reproduction could not be reflected in the SACF because the carrier frequency was desynchronized with the starts of modulating segments in our experiments. However, maxima corresponding to the period of the carrier frequency are seen in the common autocorrelation. The effect is detectable only for low-frequency peripheral neurons in amphibians and was not observed in this work. However, the common ACF showed signs of periodicity in some cases, while no periodicity was seen in the SACF (Fig. 1b). This finding possibly indicates that a constant period, which is unrelated to the period in presentation of modulating segments, is characteristic of neuronal firing. As already mentioned, this periodicity is possibly due to a short, but strictly determined refractoriness.

It is of interest to compare the behavior of the curve obtained by our method to characterize the restoration of excitability after spike generation with the autocorrelation function obtained for neuronal spiking in the absence of external stimuli. Unfortunately, such a comparison is possible only for cells with marked spontaneous activity, which account for an extremely small portion of neurons in the torus semicircularis [24]. However, the scarce available data indicate that a maximum of the ACF of spontaneous neuronal activity is directly related to a local maximum of the function that was used in this work to describe the dynamics of the postspike restoration of excitability upon presentation of sound signals.

A complex and often nonmonotonic time course of the postspike restoration of excitability can be observed in studies aimed at analyzing the parameters of spontaneous activity in cells of the auditory pathway [24, 34] and other neuronal elements of the brain [35]. It is of interest that postspike inhibition of excitability is usually short and exerts a small effect on the statistical parameters of firing in the majority of cortical neurons [10]. At the same time, a distinct local (following a short refractory period) maximum has been observed in the distribution of between-spike intervals for spontaneously active cells of the cortical representation of whiskers in rats [36]. The maximum was followed by a

local minimum in the vast majority of cases; another maximum was then sometimes seen with a subsequent slow progress to a level corresponding to the Poisson distribution. This pattern corresponds to the data shown in Fig. 4. Note that functions similar to those in Fig. 4 have been obtained in model experiments as well [37].

To conclude, the method used in this work to evaluate the postspike changes in excitability lacks most of the drawbacks that were characteristic of our earlier methods and describes the total time course of the process, including both small and large delays in the response after generation of an action potential. Note that the same approach can be used to study the responses to consecutive presentations of individual signals. It will be necessary in such a case to similarly compare the sum of autocorrelation functions over all segments presented with a function that characterizes the correlation of responses to a particualr presentation with responses to all other signal presentations.

ACKNOWLEDGMENTS

This work was supported by the Russian Foundation for Basic Research (project no. 16-04-01066).

REFERENCES

1. N. G. Bibikov, Biofizika **20**, 887 (1975).
2. R. P. Gaumond, D. O. Kim, and C. E. Molnar, J. Acoust. Soc. Am. **74**, 1392 (1983).
3. N. G. Bibikov and G. A. Ivanitskii, Biofizika **30**, 141 (1985).
4. N. G. Bibikov, Usp. Fiziol. Nauk **41** (3), 72 (2010).
5. E. de Boer and P. Kuyper, IEEE Trans. Biomed. Eng. **15**, 169 (1968).
6. J. J. Eggermont, Hear. Res. **271**, 123 (2011).
7. N. G. Bibikov, Biophysics (Moscow) **49** (1), 97 (2004).
8. S. E. Shore, Hear. Res. **82**, 31 (1995).
9. N. G. Bibikov and A. B. Dymov, Biophysics (Moscow) **52** (6), 598 (2007).
10. N. G. Bibikov and I. N. Pigarev, Ross. Fiziol. Zh. im. I. M. Sechenova **99** (3), 348 (2013).
11. D. H. Louage, M. van der Heijden, and P. X. Joris, J. Neurophysiol. **91**, 2051 (2004).
12. N. G. Bibikov, in *Neuroinformatics: Proceedings of the 14th All-Russia Conference* (MIFI-Press, Moscow, 2012), Vol. 3, p. 84.
13. N. G. Bibikov and S. V. Nizamov, Biophysics (Moscow) **54** (5), 637 (2009).
14. N. G. Bibikov, Biophysics (Moscow) **60** (3), 409 (2015).
15. N. G. Bibikov, Zh. Vyssh. Nervn. Deyat. im. I. P. Pavlova **67** (2), 218 (2017).
16. H. M. Kaplan, Proc. Fed. Am. Soc. Exp. Biol. **28**, 1541 (1969).
17. M. A. Suckow, L. A. Terril, C. F. Grigdesby, and P. A. March, Pharmacol. Biochem. Behav. **63** (1), 39 (1999).
18. M. Zimmermann, Neurosci. Lett. **73**, 1 (1987).
19. P. X. Joris, D. H. Louage, L. Cardoen, and M. van der Heijden, Hear. Res. **216–217**, 19 (2006).
20. N. G. Bibikov, Sens. Sist. **3** (3), 364 (1990).
21. N. G. Bibikov, Biophysics (Moscow) **51** (2), 277 (2006).
22. N. G. Bibikov, O. B. Ovchinnikov, and S. V. Nizamov, Biophysics (Moscow) **46** (3), 520 (2001).
23. N. G. Bibikov, Acustica **31** (2), 310 (1974).
24. N. G. Bibikov, IBRO Rep. **2**, 54 (2017).
25. J. Johnston, S. J. Griffin, and C. Baker, J. Physiol. **586**, 3493 (2008).
26. B. P. Bean, Nat. Rev. Neurosci. **8**, 451 (2007).
27. J. H. Kim, C. Kushmerick, and H. von Gersdorf, J. Neurosci. **30** (46), 15479 (2010).
28. Y. Kim and L. O. Trussell, J. Neurophys. **97** (2), 1705 (2007).
29. H. Sun and S. H. Wu, Brain Res. **1226**, 70 (2008).
30. S. Chen and Y. Yaari, J. Physiol. **586** (5), 1351 (2008).
31. N. G. Bibikov and A. B. Dymov, Sens. Sist. **23** (3), 246 (2009).
32. N. G. Bibikov, Sens. Sist. **25** (2), 131 (2011).
33. N. G. Bibikov, Neirofiziologiya (Kiev) **46** (1), 18 (2014).
34. N. G. Bibikov, Zh. Evol. Biokhim. Fiziol. **49** (6) 417 (2013).
35. C. M. Bowe, J. D. Kocsis, and S. G. Waxman, Neuroscience **21**, 585 (1987).
36. G. B. Stanley and R. M. Webber, J. Comp. Neurosci. **15**, 321 (2003).
37. W. Truccolo, U. T. Eden, M. R. Fellows, et al., J. Neurophysiol. **93**, 1074 (2005).

Translated by T. Tkacheva